İSTANBUL UNIVERSITY
CERRAHPAŞA

REVIEW
Electrica 2022; 22(2): 329-341

Research on NFTSMC Speed Control of Improved Terminal Attractor of Permanent Magnet Synchronous Motor Based on SM-MRAS

Qiao Ai, Yongjun Chen

Department of Electronic Information, Yangtze University, Jingzhou, Hubei, China

Cite this article as: Q. Ai and Y. Chen, "Research on NFTSMC speed control of improved terminal attractor of permanent magnet synchronous motor based on SM-MRAS," *Electrica.*, 22(2), 329-341, 2022.

ABSTRACT

In order to solve the problems of high cost, low reliability, unstable performance, and difficult maintenance in the complex working conditions brought about by traditional mechanical sensors to the permanent magnet synchronous motor (PMSM) control system, a continuous hyperbolic tangent function sigmoid is first proposed as the variable-structure model of the switching function. It refers to the method of the model reference adaptive system (MRAS) observer to estimate the motor speed and rotor position. Secondly, in view of the inherent chattering and poor robustness of the traditional sliding mode control (SMC), a speed-loop control strategy of nonsingular fast terminal sliding mode control (NFTSMC) is proposed. On this basis, a new type of reaching law with an improved terminal attractor that can eliminate negative exponential terms is designed. This control technology can quickly converge under conditions of sudden load changes and motor parameter changes, and improve the dynamic response of the system. Finally, simulation and experimental verification are carried out based on PSIM software and the PTS-3000 experimental platform. The results prove that MRAS positionless control can accurately estimate the rotor speed and position, and the NFTSMC based on the improved terminal attractor has superior control performance.

***Index Terms*—**Attractor with exponential term, model reference adaptation, nonsingular fast terminal sliding mode control, sliding mode control

I. INTRODUCTION

Owing to their simple structure, reliable operation, high transmission efficiency, good heat dissipation, small size, and easy manual maintenance, permanent magnet synchronous motors (PMSMs) are widely used in small and medium powered high-precision speed and position control systems [1]. When using magnetic field vector-oriented control, it is necessary to obtain accurate rotor position information and speed information in order to achieve high performance of the three-phase PMSM. Generally, the encoder is used to measure the speed and position of the rotor, but the installation and use of the encoder will increase the cost of the system, reduce the anti-interference ability of the system. Moreover, it is not easy to repair under many actual working conditions. In order to solve this problem, many scholars have developed research on sensorless control technology, such as the flux estimation method, the extended Kalman filter method, the model reference adaptive method [2, 3], etc. The model reference adaptive system (MRAS) has been widely used in the industry due to the practicality and simplicity of its algorithm. The difficulty lies in the establishment of the reference model and the adjustable model of the control system, so that the output of the two physical quantities has the same meaning. When there is an error between the two models, an appropriate adaptive rate should be designed to make the estimated parameters of the adjustable model gradually approach. Refer to the actual parameters of the model until the error between the two is less than a certain minimum threshold of the desired parameter target.

Linear proportional integral (PI) control is widely used in the field of motor drives because of its simple implementation method [4]. However, PMSM is a complex multi-dimensional system. When the control system is disturbed by the external or the internal parameters and the loads are changed, the traditional PI control cannot meet the requirements of all actual working conditions. In view of the various parameter uncertainties and nonlinearities of PMSMs, researchers have proposed many different nonlinear control techniques to achieve high performance control, such as robust control [5], terminal sliding mode (TSMC) control [6], neural network control

Corresponding Author: Yongjun Chen

E-mail: yj_ch@163.com

Received: May 25, 2021

Revised: November 13, 2021

Accepted: November 23, 2021

DOI: 10.54614/electrica.2022.210055

[7], active disturbance rejection control [8], etc. Among them, sliding mode control (SMC) is a type of variable-structure system, whose theory was originated by Professor Utkin and Professor Emelyanov of the former Soviet Union in the late 1950s [9, 10], It does not require high model accuracy and has strong robustness to internal and external disturbances. Therefore, it is given a priority in the field of motor drives. So far, SMC has been widely used in the field of servo control, including terminal SMC. It has become a research hotspot of SMC technology, because of its advantages of fast convergence in finite time,

The difficulty of TSMC lies in the singularity of the control law. When the state of the system approaches zero infinitely, the negative exponential term of the state in the control law will cause the control quantity to tend to infinity, resulting in singularities. In response to this problem, the authors in [11, 12] proposed a nonsingular terminal sliding mode control to make the state of the sliding phase converge in a finite time, in which the control law has no negative exponential term. However, this method has a slower convergence speed in the region far from the equilibrium point, and the inherent chattering phenomenon of SMC has not been significantly improved. In [13], the authors proposed nonsingular fast terminal sliding mode control (NFTSMC) to achieve rapid convergence when the system state is far from the equilibrium point. In [14, 15], the authors proposed adaptive SMC technology to eliminate chattering. In [16], a continuous fast terminal sliding mode control (CFTSMC) is proposed to solve the chattering phenomenon and improve the robustness of the system. However, the CFTSMC method requires a higher switching gain under strong disturbances; as a result, the speed of the permanent magnet synchronous motor has large chattering and oscillation, and the anti-interference ability of the system becomes worse. Based on [17], a composite CFTSMC technology based on ESO is proposed. The system disturbance observed by ESO is used for feedforward compensation, which can reduce the influence of disturbance and reduce the speed oscillation. However, there are too many ESO parameters and it is difficult to set. In [18], an adaptive terminal sliding mode reaching law (ATSMRL) with CFTSMC is proposed, to improve the dynamic performance of the PMSM drive system. The proposed ATSMRL arrival law can improve the performance of the arrival time and effectively reduce the jitter of the control system.

Based on the above research, this paper proposes an improved nonsingular fast terminal control with exponential term attractor, which realizes continuous input time, introduces the fast terminal reaching law, and improves the original linear or exponential reaching law to make it faster. The approach of the terminal improves the approach speed of the system state and improves the anti-interference ability of the system. Finally, simulation and experimental verification are carried out based on PSIM software and the PTS-3000 experimental platform, and results consistent with the theory are obtained.

II. MODEL REFERENCE ADAPTIVE SYSTEM CONTROL MODEL

A. The Mathematical Model of the Permanent Magnet Synchronous Motor

Following the assumptions of a series of ideal motor models, the mathematical model of the three-phase PMSM in the synchronously rotating d-q coordinate system can be derived through the principle of coordinate transformation.

$$\begin{cases} U_d = Ri_d + L_d \dfrac{d}{dt} i_q - \omega_e L_q i_q \\ U_q = Ri_q + L_q \dfrac{d}{dt} i_q + \omega_e \left(L_d i_d + \varphi_f \right) \\ T_e = \dfrac{3}{2} n_p \left(\varphi_f i_q + \left(L_d - L_q \right) i_d i_q \right) \\ T_e - T_L = \dfrac{1}{n_p} J \dfrac{d\omega_r}{dt} + B \dfrac{\omega_r}{n_p} \end{cases} \tag{1}$$

In the formula, if U_d, U_q are the direct and quadrature axis voltages; i_d, i_q are the direct and quadrature axis currents; ω_r is the mechanical angular velocity of the motor; ω_e is the electrical angular velocity of the motor's rotor; n_p is the number of pole pairs of the motor; φ_f is the rotor flux; R_s is the stator winding resistance; J is the moment of inertia; B is the damping coefficient; and $L_d = L_q = L_s$ is the equivalent inductance of the stator winding; then, $T_e = 1.5 n_p \varphi_f i_q$ It can be seen that the electromagnetic torque and the quadrature axis current have a linear relationship, and the linear control of the PMSM torque can be achieved by controlling i_q.

Aiming at the shortcoming of the traditional MRAS observer's strong dependence on PMSM parameters and the shortcoming of large jitter of the commonly used symbol switching functions in the variable structure, this paper designs a variable-structure MRAS observer with the continuous hyperbolic tangent function sigmoid as the switching function. The system speed dynamic response is fast, the rotor position error is small, and it has strong robustness to motor parameter changes and disturbances. The reference model in the current equation, as shown in (2), is the current state equation of the three-phase surface-mount PMSM in the rotating coordinate system,

$$\begin{cases} \dfrac{d}{dt} i_d = -\dfrac{R}{L_s} i_d + \omega_e i_q + \dfrac{1}{L_s} U_d \\ \dfrac{d}{dt} i_q = -\dfrac{R}{L_s} i_q - \omega_e i_d - \dfrac{\varphi_f}{L_s} \omega_e + \dfrac{1}{L_s} U_d \end{cases} \tag{2}$$

Rewriting the current state equation,

$$\begin{cases} \dfrac{d}{dt} \left(i_d + \dfrac{\varphi_f}{L_s} \right) = -\dfrac{R}{L_s} \left(i_d + \dfrac{\varphi_f}{L_s} \right) + \omega_e i_q + \dfrac{1}{L_s} \left(U_d + \dfrac{R\varphi_f}{L_S} \right) \\ \dfrac{d}{dt} i_q = -\dfrac{R}{L} i_q - \omega_e \left(i_d + \dfrac{\varphi_f}{L_s} \right) + \dfrac{1}{L_s} U_q \end{cases} \tag{3}$$

Definition

$$\begin{cases} i_d^{'} = i_d + \dfrac{\varphi_f}{L_s} \\ i_q^{'} = i_q \\ U_d^{'} = U_d + \dfrac{R}{L_s} \varphi_f \\ U_q^{'} = U_q \end{cases} \tag{4}$$

Then, (2) can become

$$\begin{cases} \frac{d}{dt}i_d^{'} = -\frac{R}{L_s}i_d^{'} + \omega_e i_q^{'} + \frac{1}{L_s}U_d^{'} \\ \frac{d}{dt}i_q^{'} = -\frac{R}{L_s}i_q^{'} - \omega_e i_d^{'} + \frac{1}{L_s}U_q^{'} \end{cases}. \tag{5}$$

Write (5) as the space state equation

$$\frac{d}{dt}i^{'} = Ai^{'} + Bu^{'}. \tag{6}$$

Among them, $i^{'} = \begin{bmatrix} i_d^{'} \\ i_q^{'} \end{bmatrix}$, $U^{'} = \begin{bmatrix} U_d^{'} \\ U_q^{'} \end{bmatrix}$ $A = \begin{bmatrix} -\frac{R}{L_s} & \omega_e \\ \omega_e & -\frac{R}{L_s} \end{bmatrix}$, $B = \begin{bmatrix} \frac{1}{L_s} & 0 \\ 0 & \frac{1}{L_s} \end{bmatrix}$. The above formula A contains rotor speed information, and (6) can be used as an adjustable model, where ω_e is the adjustable parameter to be identified.

Using the estimated value expression (5), we get

$$\begin{cases} \frac{d}{dt}\breve{i}_d^{'} = -\frac{R}{L_s}\breve{i}_d^{'} + \omega_e \breve{i}_q^{'} + \frac{1}{L_s}U_d^{'} \\ \frac{d}{dt}\breve{i}_q^{'} = -\frac{R}{L_s}\breve{i}_q^{'} - \omega_e \breve{i}_d^{'} + \frac{1}{L_s}U_q^{'} \end{cases}. \tag{7}$$

Also, writing the above equation as the space state equation

$$\frac{d}{dt}\breve{i}^{'} = \breve{A}\breve{i}^{'} + BU^{'}. \tag{8}$$

Among them, $\breve{i}^{'} = \begin{bmatrix} \breve{i}_d^{'} \\ \breve{i}_q^{'} \end{bmatrix}$, $\breve{A} = \begin{bmatrix} -\frac{R}{L_s} & \breve{\omega}_e \\ -\breve{\omega}_e & -\frac{R}{L_s} \end{bmatrix}$. Defining generalized error,

$$err = i^{'} - \breve{i}^{'}. \tag{9}$$

The state equation of current error can be obtained by subtracting (7) from (5)

$$\frac{d}{dt}\begin{bmatrix} \widetilde{err}_d \\ \widetilde{err}_q \end{bmatrix} = \begin{bmatrix} -\frac{R}{L_s} & \omega_e \\ \omega_e & -\frac{R}{L_s} \end{bmatrix}\begin{bmatrix} \widetilde{err}_d \\ \widetilde{err}_q \end{bmatrix} - J\left(\omega_e - \breve{\omega}_e\right)\begin{bmatrix} \breve{i}_d^{'} \\ \breve{i}_q^{'} \end{bmatrix}. \tag{10}$$

Among them, $J = \begin{bmatrix} 0 & -1 \\ 1 & 0 \end{bmatrix}$ rewritten into space state equation

$$\frac{d}{dt}err = Aerr - W. \tag{11}$$

Among them, $W = J\left(\omega_e - \breve{\omega}_e\right)\breve{i}^{'}$.

Popov's theory of hyperstability is used for analysis, and the entire control system can be gradually stabilized when the following two conditions are met simultaneously:

1) The transfer matrix $H(s) = (sI - A)^{-1}$ is a strictly positive definite matrix.

2) If $\eta(0,t_1) = \int_0^{t_1} V^T W dt \geq -\gamma_0^2, \forall t_1 \geq 0, \gamma_0$ is any finite number, $\lim_{t\to\infty} err(t) = 0$ means MRAS is gradually stable.

B. Traditional Model Reference Adaptive System Observer

The adaptive rate can be obtained by solving Popov's integral inequality inversely. The MRAS generally uses a PI controller, which can be obtained by

$$\breve{\omega}_e = \int_0^t K_i\left(i_d^{'}\breve{i}_q^{'} - \breve{i}_d^{'}i_q^{'}\right)d\tau + K_p\left(i_d^{'}\breve{i}_q^{'} - \breve{i}_d^{'}i_q^{'}\right) \tag{12}$$

$$\breve{\omega}_e = \left(\frac{K_i}{s} + K_p\right)err_\omega. \tag{13}$$

Among them,

$$err_\omega = i_d^{'}\breve{i}_q^{'} - \breve{i}_d^{'}i_q^{'} = i^{'} \times \breve{i}^{'}. \tag{14}$$

Substituting (4) into (12), we can get

$$\breve{\omega}_e = \left(\frac{K_i}{s} + K_p\right)\left[i_d\breve{i}_q - \breve{i}_d i_q - \frac{\varphi_f}{L_s}\left(i_q - \breve{i}_q\right)\right]. \tag{15}$$

Integrate (15) to get the estimated value of rotor position

$$\breve{\theta}_e = \int \breve{\omega}_e d\tau. \tag{16}$$

C. Variable-Structure Model Reference Adaptive System Observer

Sliding mode control has a switching characteristic that allows the system structure to change with time. This characteristic allows the system to move up and down along a prescribed state track with a smaller amplitude and a higher frequency under certain conditions, usually called "sliding mode." The sliding mode can be designed according to actual needs, and has nothing to do with system parameters and external interference. Thus, the control system in the sliding mode is very strong and robust, and its movement process is shown in Fig. 1.

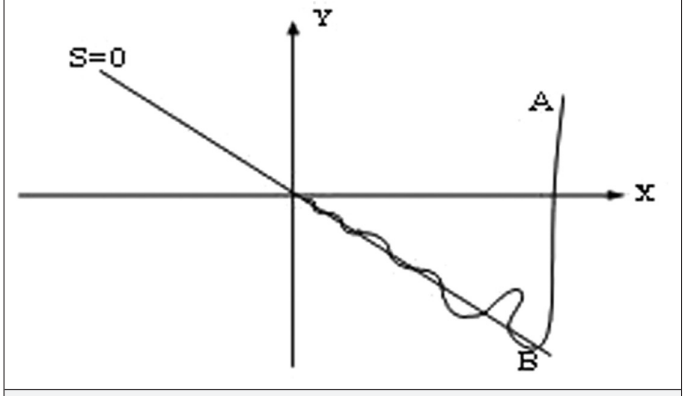

Fig. 1. The two motion stages of a sliding mode control system.

The principle of variable-structure MRAS is to use the sliding mode variable-structure theory to find the equivalent speed, so that the actual motor speed affected by random and uncertain factors can follow the given speed, namely

$$\lim_{t\to 0} err(t) = 0. \tag{17}$$

The design of the sliding mode variable-structure observer includes two parts, namely, the selection of sliding mode surface and the design of control law.

The principle of constructing the sliding surface is that it is progressively stable when the system is sliding and has a good dynamic response. The switching function equation for constructing the sliding mode MRAS observer is

$$s = \left[i_d \check{i}_q - \check{i}_d i_q - \frac{\varphi_f}{L_s}\left(i_q - \check{i}_q\right) \right]. \tag{18}$$

Differentiate it to get

$$\dot{s} = \dot{i}_d \check{i}_q + i_d \dot{\check{i}}_q - \dot{\check{i}}_d i_q - \check{i}_d \dot{i}_q - \frac{\varphi_f (\dot{i}_q - \dot{\check{i}}_q)}{L_s}. \tag{19}$$

According to the basic idea of sliding mode variable-structure control, when the sliding mode enters the sliding mode surface, the equivalent velocity expression can be obtained according to $s = \dot{s} = 0$,

$$\omega_{eq} = \omega + \frac{\frac{2R}{L_s}(\check{i}_d i_q - \check{i}_q i_d) + \frac{U_q}{L_s}(i_d - \check{i}_d) + (\frac{R\varphi_f}{L_s{}^2} - \frac{U_d}{L_s})(i_q - \check{i}_q)}{\check{i}_d i_q + \check{i}_q i_d + \frac{\varphi_f (i_d + \check{i}_d)}{L_s} + (\frac{\varphi_f}{L_s})^2}. \tag{20}$$

It can be seen from (20) that when the estimated current converges to the reference current, the estimated speed converges to the actual speed, that is, $\dot{i} = \dot{i}$ when $\omega_{eq} = \omega$.

The conventional sliding mode variable-structure control design method has constant value switching between control, function switching control, and proportional switching control.

In this paper, constant switching control is adopted, and the velocity estimation expression of the traditional MRAS observer is as follows

$$\check{\omega}_e = K sign(s). \tag{21}$$

In order to solve the chattering of the system caused by the discontinuity of the switching characteristics of the traditional sliding mode meter structure, a quasi-sliding mode is introduced into the SMC, and the hyperbolic tangent continuous function sigmoid is used instead of the sign function to reduce the filtering link. The speed of the improved MRAS observer is estimated as

$$\check{\omega}_e = KH(s). \tag{22}$$

Among them, *H*(*s*) is the hyperbolic tangent continuous function, and the expression is as follows

$$H(s) = \frac{2}{1+e^{-s}} - 1. \tag{23}$$

The control block diagram of the improved sliding mode MRAS observer is as follows:

D. Stability Analysis

The motion of the sliding mode variable -structure control system consists of approaching motion and sliding mode motion composition, as long as the system can approach and enter the sliding mode at the arrival stage, and the sliding stage remains stable, that is, satisfies the existence condition of the generalized sliding mode. In order to analyze the stability of the observer, the Lyapunov function is defined as

$$V(x) = \frac{1}{2}s^2, s \neq 0 \tag{24}$$

and its derivative is

$$\dot{V}(x) = s\dot{s}, s \neq 0. \tag{25}$$

That is, the condition for the system sliding mode to exist and reach the sliding mode surface is

$$\dot{V}(x) = s\dot{s} < 0, \text{且} \lim_{x\to\infty} s = 0 \tag{26}$$

From (4), (19), and (20), we can get

$$\begin{aligned} \dot{s} = {} & \omega\left[i_d \check{i}_d + i_q \check{i}_q + \frac{\varphi_f}{L_s}\check{i}_d + \frac{\varphi_f}{L_s}\check{i}_q + (\frac{\varphi_f}{L_s})^2 \right] \\ & .-\check{\omega}\left[i_d \check{i}_d + i_q \check{i}_q + \frac{\varphi_f}{L_s}\check{i}_d + \frac{\varphi_f}{L_s}\check{i}_q + (\frac{\varphi_f}{L_s})^2 \right] \\ & +\left[\frac{2R}{L_s}(\check{i}_d i_q - \check{i}_q i_d) + \frac{U_q}{L_s}(i_d - \check{i}_d) + (\frac{R\varphi_f}{L_s{}^2} - \frac{U_d}{L_s})(i_q - \check{i}_q) \right] \end{aligned} . \tag{27}$$

Then, (27) can become

$$\begin{aligned} \dot{s} = {} & F(i_d, \check{i}_d, i_q, \check{i}_q, U_d, U_q, L_s, R, \varphi_f, \omega) \\ & -K\left[i_d \check{i}_d + i_q \check{i}_q + \frac{\varphi_f}{L_s}\check{i}_d + \frac{\varphi_f}{L_s} i_d + (\frac{\varphi_f}{L_s})^2 \right] sign(s) \end{aligned} . \tag{28}$$

F is a bounded function, and there must be an upper limit, which can be known when the motor runs normally, as

$$i_d \check{i}_d + i_q \check{i}_q + \frac{\varphi_f}{L_s}\check{i}_d + \frac{\varphi_f}{L_s} i_d + (\frac{\varphi_f}{L_s})^2 > 0 . \tag{29}$$

Then, there must be a sufficiently large *K* so that the switching surface has the ability to attract all the moving points in a certain area, that is, it should satisfy

$$\lim_{s\to 0^+} \dot{s} < 0 \text{及} \lim_{s\to 0^-} \dot{s} > 0 \text{或} s\dot{s} < 0. \tag{30}$$

When the system state enters the sliding mode surface, that is, when $s = \dot{s} = 0$, the estimated speed converges to the actual speed, and the system is stable.

E. The Design of the Speed Controller

Terminal sliding mode control (TSMC) has been widely used in the field of motor control due to the introduction of nonlinear terms in the design of the sliding mode surface, so that the system state can converge to the equilibrium point in a finite time. However, when

the system state is close to zero, the control amount of the traditional TSMC may tend to infinity, that is, a singular phenomenon appears, and the chattering phenomenon cannot be eliminated, which greatly limits the further development of TSMC. It is to solve this problem that NTFSMC came into being. It inherits the advantages of traditional TSMC convergence in finite time. At the same time, because there is no negative exponential term in the control law, the singularity is fundamentally eliminated. It also solves the problem of slow convergence when the state variable is far from the equilibrium point.

F. A Nonsingular Fast Terminal Sliding Surface Design

The input of the degree controller is the rotational speed error, and the output is the given amount of q-axis current i_q^* which is used to accurately track the given speed and is robust to load and some uncertain disturbances. Suppose the speed reference signal is ω_{ref} and the difference between the speed reference value and the actual value is defined as a state variable, $x_1=\omega_{ref}-\omega_r$, $x_1=x_2$ can be obtained.

The mathematical function of the traditional nonsingular terminal sliding mode surface is

$$s = x_1 + \frac{1}{\beta} x_2^{p/q} . \tag{31}$$

Among them, p and q are odd numbers and satisfy $1 < p/q < 2$.

The nonsingular fast terminal sliding surface proposed in this paper is

$$s = cx_1 + \frac{1}{\beta} x_2{}^{p/q} + \frac{1}{\alpha} x_1^{g/h} . \tag{32}$$

Among them, $\alpha \in R^+$, $\beta \in R^+$, p, q, g, $h \in N$ are odd numbers, and $1 < p/q < 2$, $g/h > p/q$.

In order to completely eliminate the nonlinear switching term in the control law and avoid system chattering, the attractor is usually used to design the SMC law. Among them, the terminal attractor can make the state reach the sliding mode surface in a limited time, and has good robustness to model misunderstanding and external interference, and is widely used in SMC. The traditional terminal attractor is as follows:

$$\dot{s} = -\phi s - \gamma s^{m/n} . \tag{33}$$

The control law of the new nonsingular sliding mode controller for the speed loop is

$$u = \frac{\beta q}{p} x_2^{1-p/q} \left[\left(\phi s + \gamma s^{m/n} \right) + x_2 \left(c + \frac{g}{\alpha h} x_1^{g/h-1} \right) \right]. \tag{34}$$

Based on the characteristics of NTFSMC, this article adds $x_2^{p/q-1}$ to obtain a new attractor on the basis of the traditional terminal attractor,

$$\dot{s} = \left(-\phi s - \gamma s^{m/n} \right) x_2^{p/q-1} \tag{35}$$

From the above, the control law of the new nonsingular sliding mode controller for the speed loop is

$$u = \frac{\beta q}{p} \left[\left(\phi s + \gamma s^{m/n} \right) + x_2^{2-p/q} \left(c + \frac{g}{\alpha h} x_1^{g/h-1} \right) \right]. \tag{36}$$

In (37), the exponents of the state variables x_1 and x_2 are all at zero, and there is no negative exponential term. This shows that the SMC method, based on NTFSMC and the improved terminal attractor, completely avoids the singularity problem, and the control law time is continuous chattering. In addition, compared with the traditional terminal SMC law, the x_2 exponential term in the control law (u) contains the factor of state x_1. When the system state x is far from the equilibrium point $x=0$, this factor has the effect of increasing the control quantity, thereby improving the closed-loop system convergence rate. When the system state is close to the equilibrium point $x=0$, the factor is approximately 1, and the control law (u) is approximately the general terminal SMC law, which ensures that it has almost the same robust performance to model errors and external interference.

G. Speed Controller Design

From the foregoing, it can be seen that the PMSM system state variables are defined as follows:

$$\begin{cases} x_1 = \omega_{ref} - \omega_r \\ x_2 = \dot{x}_1 = -\dot{\omega}_r \end{cases} . \tag{37}$$

Among them, ω_{ref} is the reference speed of the PMSM, usually a constant, and ω_r is the actual speed of the PMSM. According to (1), we can see

$$\begin{cases} \dot{x}_1 = -\dfrac{d\omega_r}{dt} = -\dfrac{p_n}{J}\left(\dfrac{3}{2} p_n \phi_f i_q - T_L\right) \\ \dot{x}_2 = -\dfrac{d^2\omega_r}{dt} = -\dfrac{3}{2J} p_n{}^2 \phi_f \dfrac{di_q}{dt} \end{cases} . \tag{38}$$

Let $D = \dfrac{3p_n{}^2\phi_f}{2J}$, $u = \dfrac{di_q}{dt}$, then (38) can be changed to

$$\begin{bmatrix} \dot{x}_1 \\ \dot{x}_2 \end{bmatrix} = \begin{bmatrix} 0 & 1 \\ 0 & 0 \end{bmatrix} \begin{bmatrix} x_1 \\ x_2 \end{bmatrix} + \begin{bmatrix} 0 \\ -D \end{bmatrix} u . \tag{39}$$

The integral sliding mode surface can smoothen torque, weaken chattering, eliminate system steady-state errors, and improve the dynamic quality of the system. Selecting (35) as the sliding surface, combining (36) and (39), the q-axis reference current can be obtained as

$$i_q^* = \frac{1}{D} \int \left[\frac{\beta q}{p} \left[\left(\phi s + \gamma s^{m/n} \right) + x_2^{2-p/q} \left(c + \frac{g}{\alpha h} x_1^{g/h-1} \right) \right] \right] dt . \tag{40}$$

III. SIMULATION AND EXPERIMENTAL RESEARCH

A. Simulation Results and Discussion

In order to verify the feasibility and superiority of the control algorithm proposed in this paper, the overall simulation control model of the PMSM control system was built in the PSIM software, and the corresponding simulation was verified.

Power simulation (PSIM) is an application and practical simulation software launched by Powersim Inc., an American company for power electronics, power conversion systems, and motor drives. It is simple and easy to use, with fast simulation speed, powerful graphical interface, and convergence. Besides its robustness and other

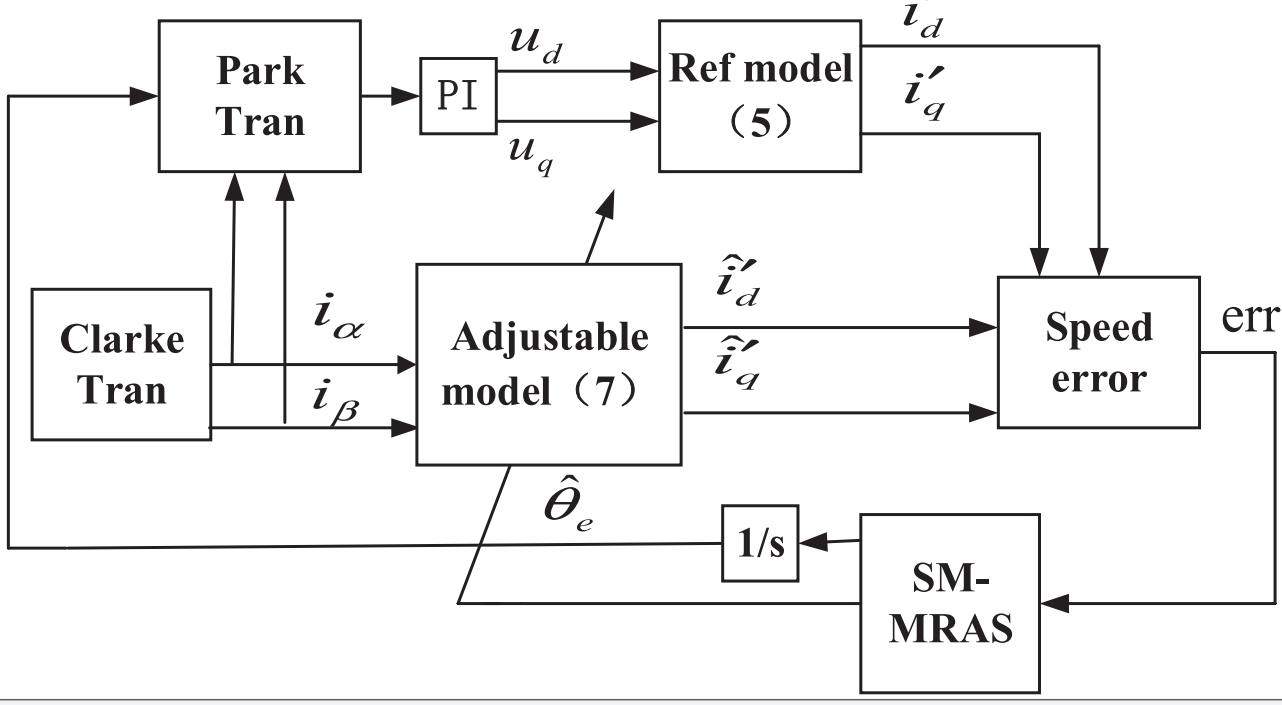

Fig. 2. MRAS control principle diagram.

advantages, it can provide powerful help for users to quickly design and develop power electronic equipment, greatly shortening the usage time.

Simulation condition setting: DC bus side voltage is 100V, PWM switching frequency is 20 kHz, simulation time is set to 1.2 seconds, reference speed is 800 r/minute, sudden load increase at 0.5 seconds, sudden load reduction at 0.8 seconds, and the specific simulation results are as follows.

B. System Response Under Sudden Load Changes

It can be seen from Fig. 3–6 that the system quickly converges to the given speed in a short period of time, and there is almost no overshoot. When the torque load changes, the NFTSMC, based on the improved terminal attractor proposed in this paper, has smaller speed fluctuations and shorter recovery time than traditional SMC control, improved SMC, and NTSMC based on the traditional terminal attractor. The torque response and current response of the control method are sensitive to load changes, but the dynamic performance of the control strategy in this paper is relatively good.

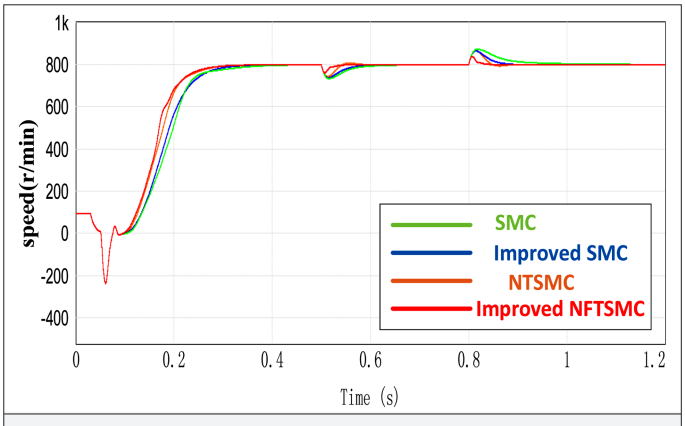

Fig. 3. Speed response curve under sudden load change.

C. The System Response Under the Change of the Internal Parameters of the Motor

Aiming at the situation that the internal parameters of the motor will change during operation under actual working conditions, this paper simulates the situation when the rotational inertia and rotor resistance change, to test the robustness of the designed control system.

In order to fully compare the speed performance under the condition of inertial mismatch, simulations were carried out on four

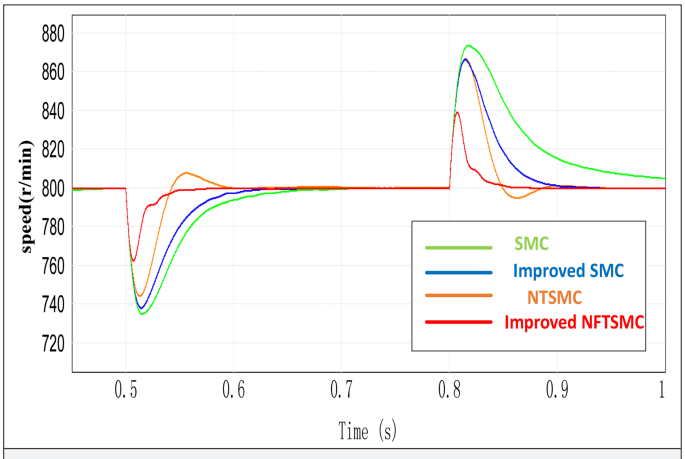

Fig. 4. Local amplification speed response curve under sudden load change.

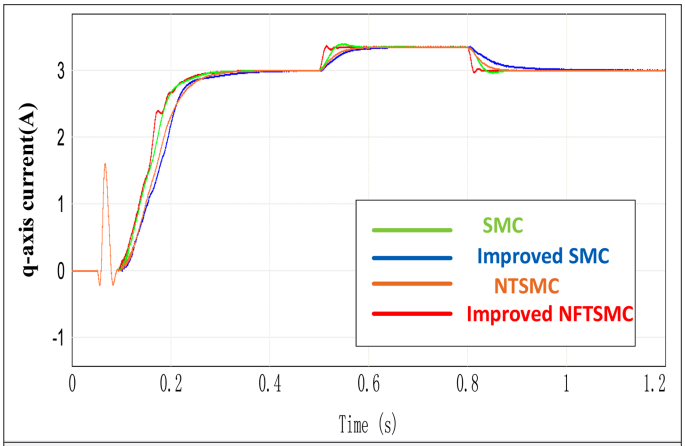

Fig. 5. q-Axis response curve under sudden load change.

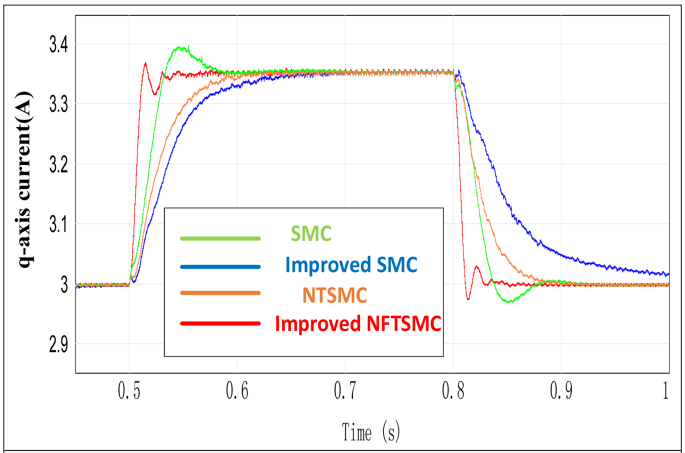

Fig. 6. Partially enlarged q-axis response curve under sudden load change.

control methods based on the traditional SMC, improved SMC, traditional NTSMC, and NFTSMC based on the improved terminal attractor. It can be seen from Fig. 7 to 10 that in the improved terminal, when the inertia of the attractor at half and double (0.5 J and 2 J) of the NFTSMC does not match, the dynamic response of the system is fast and the steady-state error is small, which further illustrates the superiority of the control algorithm proposed in this paper.

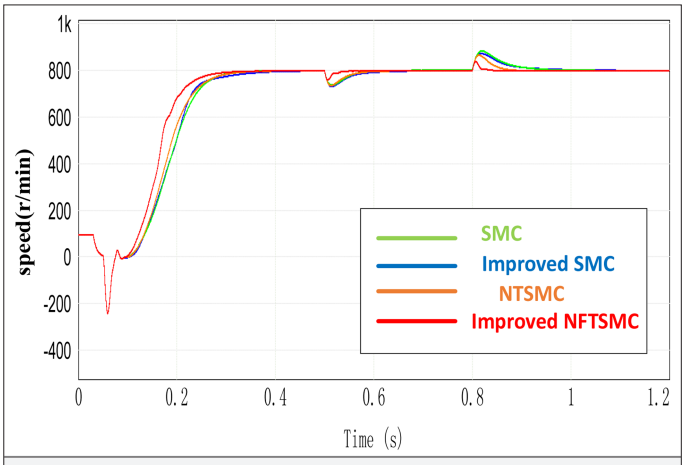

Fig. 7. Speed response curve under 0.5 J.

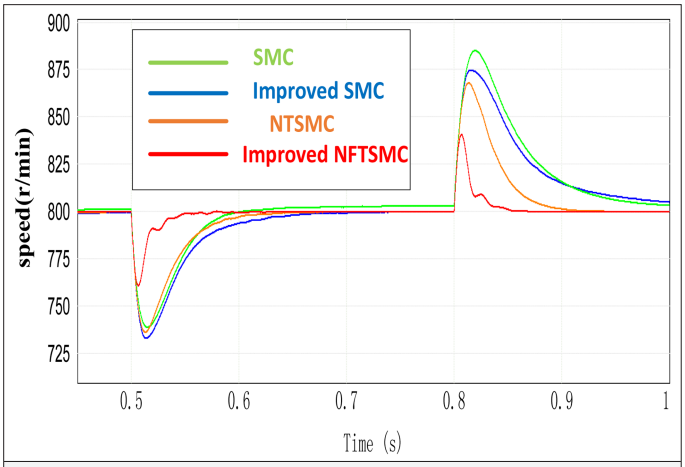

Fig. 8. Partially enlarged velocity response curve under 0.5 J.

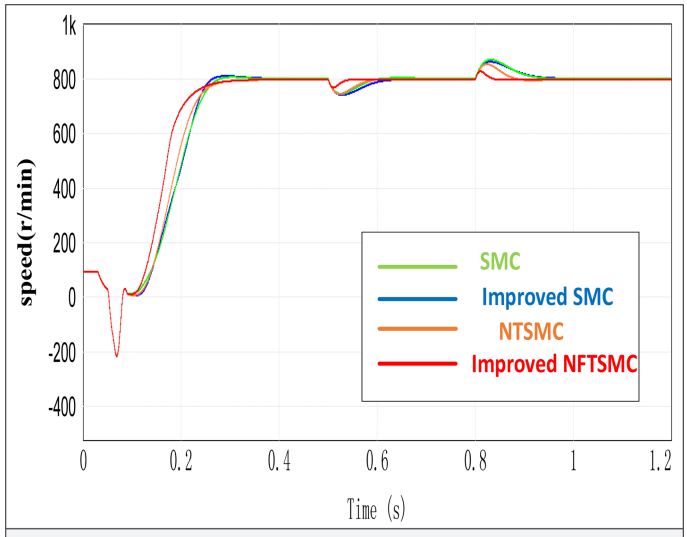

Fig. 9. Speed response curve under 2 J.

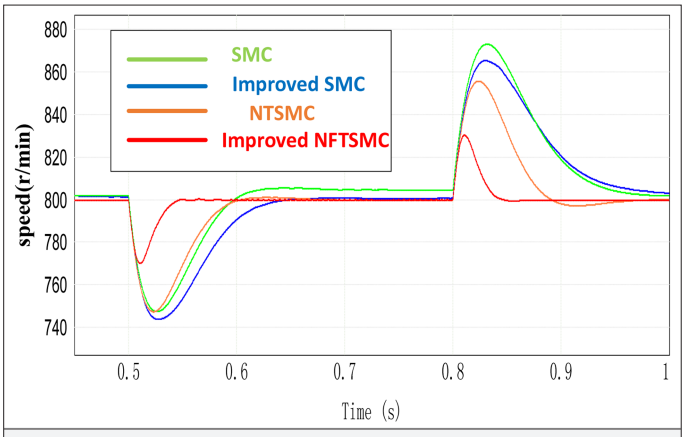

Fig. 10. Partially enlarged velocity response curve under 2 J.

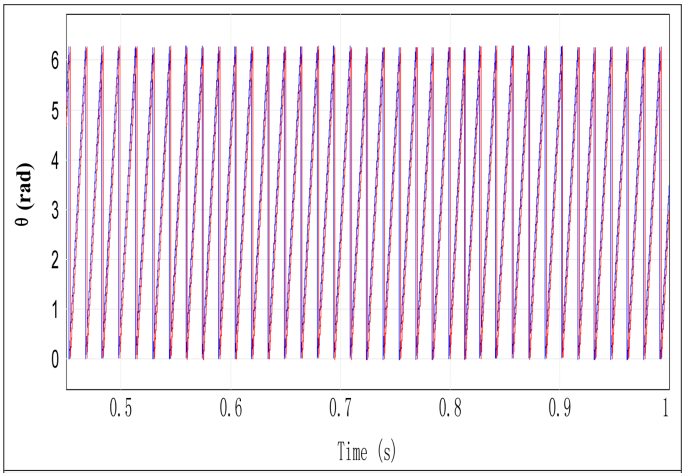

Fig. 11. Rotor position estimation curve.

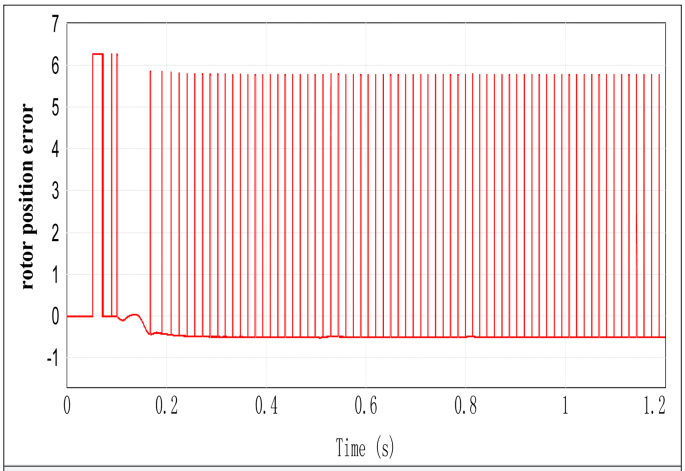

Fig. 12. Rotor position error curve.

D. Model Reference Adaptive System Algorithm Simulation

Fig. 11 is a graph of actual rotor position and estimated rotor position. Due to the fast speed and dense position waveforms, a partial enlarged view is used. Fig. 12 is a graph of the error between the actual rotor position and the estimated rotor position, and Fig. 13 and 14 are the difference between the actual speed and the estimated speed of the PMSM. It can be seen from Fig. 13 and 14 that the rotor speeds can follow the actual speed of the PMSM well, except for the short-term error during the start and acceleration of the motor. It can be seen from the above that the accuracy and feasibility of the MRAS design in this paper are proved, and the limitation brought by the encoder is solved to a certain extent.

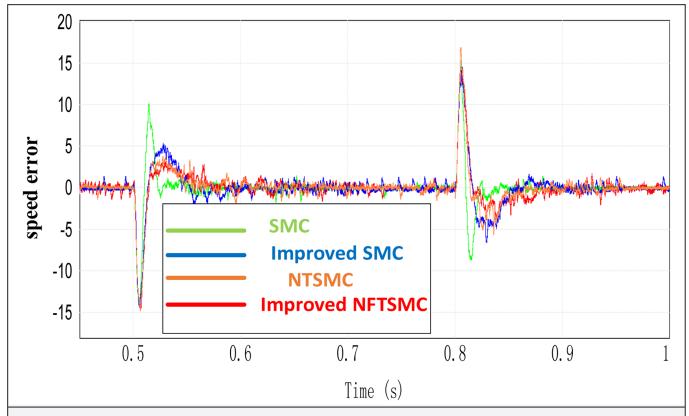

Fig. 14. Partially enlarged speed error curve.

E. Experimental Results and Discussion

In order to further verify the accuracy of the algorithm proposed in this article, on the PTS3000 experimental platform, a physical system was built with TI's special motor controller TMS320F28335 DSP for experimental verification. The TMS320F28335 involves multiple channels of 16-bit pulse-width modulators (HR-EPWM) with a high-resolution 8-bit part, with probability to arrange the PWM in the remainder of the digital clock ("micro-steps"). Such PWMs work at clock high frequencies and can be used as precise digital-to-analog converters.The motor parameters and the controller parameters are the same as in the simulation. The diagram of the experiment is as follows:

The specific experimental results are as follows:

F. A Velocity Loop Experiment

The motor speed given in this experiment is 800 r/min, and the given speed is increased to 1000 r/min in 0.5 seconds, and then the speed is restored to 800 r/min, and the given speed is suddenly reduced to

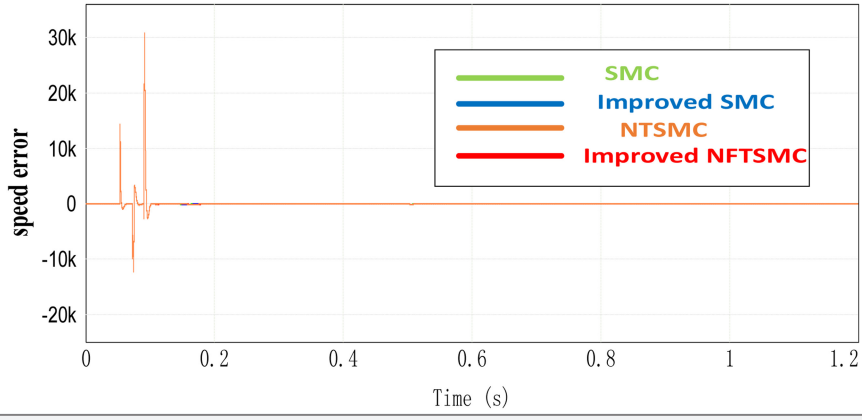

Fig. 13. Speed following error curve.

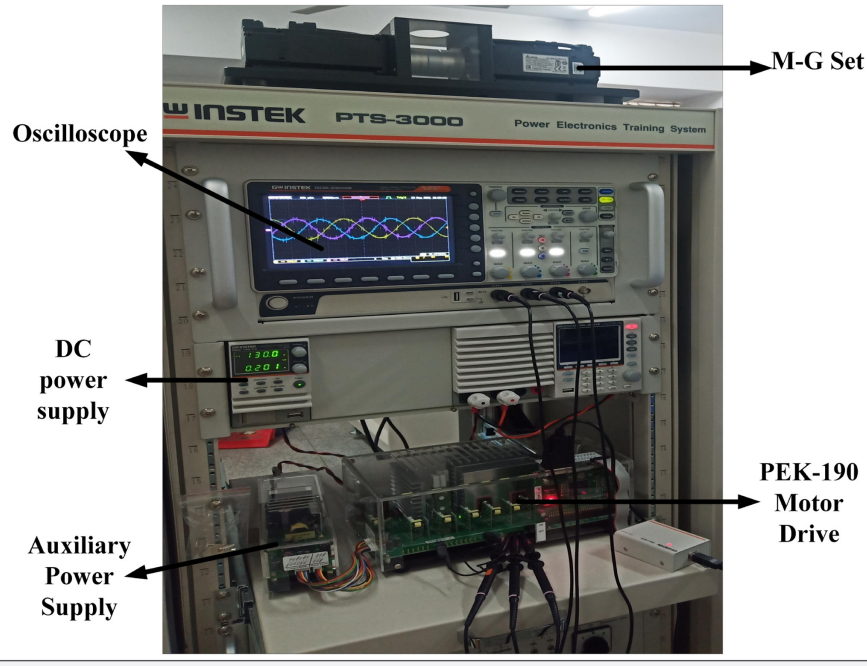

Fig. 15. Experimental wiring diagram.

600 r/min at 0.8 seconds. It can be seen from Figs. 16 and 17 that the motor speed can smoothly follow the given speed in a short period of time, and the speed will not jump, which is beneficial to prolong the life of the motor. The experiment shows that the dynamic response of the system is fast and the steady-state error is small. It further illustrates the superiority of the control algorithm proposed in this paper, and the results consistent with the simulation are obtained.

G. Model Reference Adaptive System Algorithm Experiment

Fig. 18 is a graph of the actual speed of the PMSM and the estimated speed. Although there is a certain error between the two, the estimated speed of the motor can basically track the actual speed of the PMSM well, because the error is within 10 r/min. From Figs. 19 and 20, it can be seen that the position-sensorless vector control system based on the variable-structure model reference adaptive observer speed estimation algorithm can achieve better speed with closed-loop control, the error between the estimated speed and the actual speed is small, and the degree of agreement is high. The response speed is fast, and the ability to resist external interference is strong. The rotor position estimation accuracy is high, which can meet the needs of many position-sensorless controls, which further proves the accuracy and feasibility of the variable-structure MRAS design, and to a certain extent solves the limitations brought by the encoder.

IV. CONCLUSION

Aiming at the shortcomings of traditional MRAS velocity observers that are strongly dependent on PMSM parameters and the

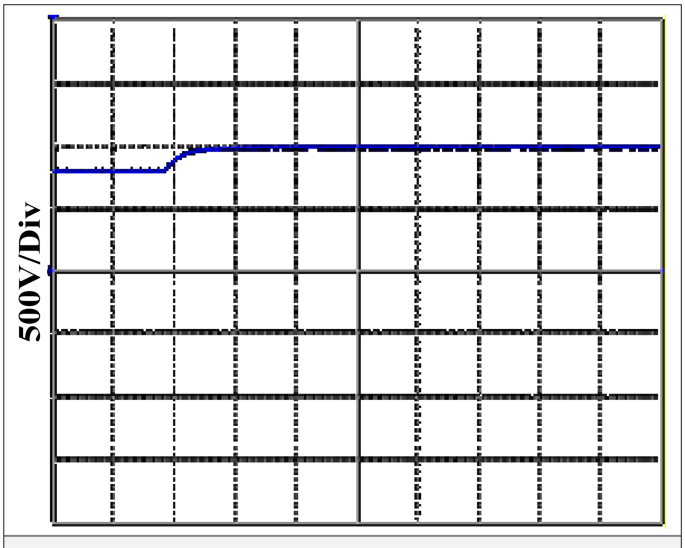

Fig. 16. Curve for suddenly increased speed.

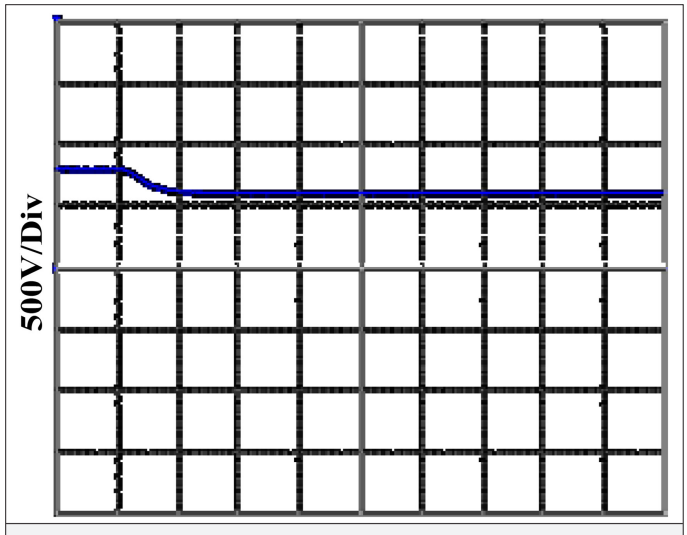

Fig. 17. Curve for suddenly decreased speed.

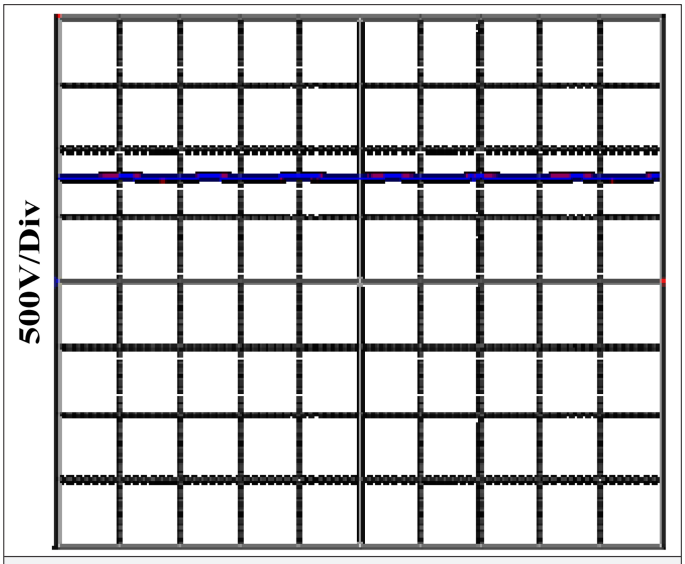

Fig. 18. Speed follow curve.

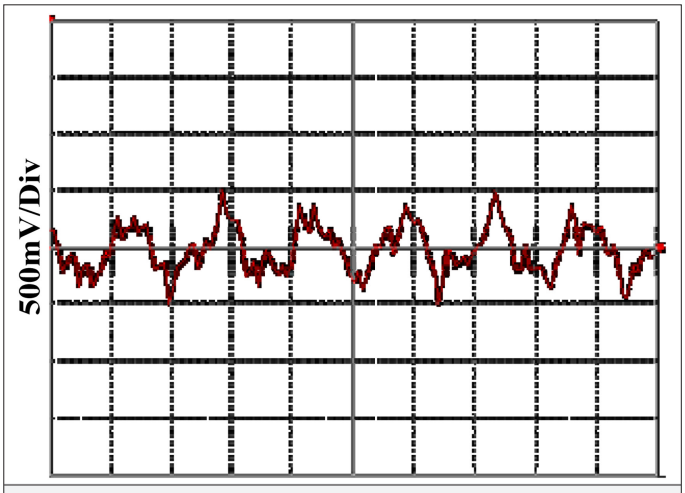

Fig. 19. Error curve.

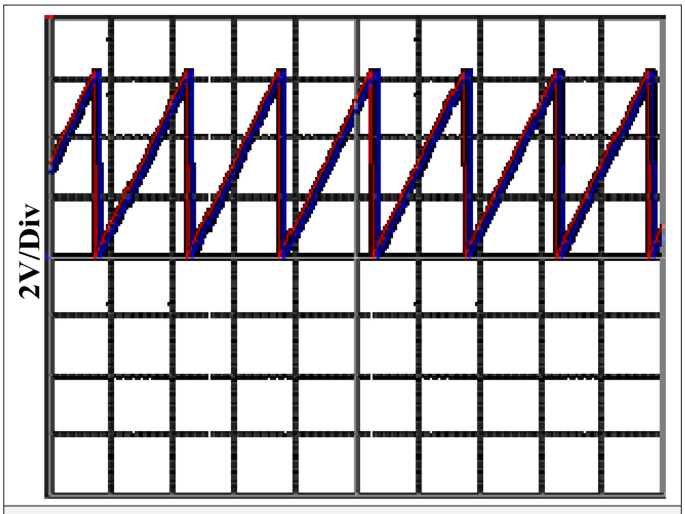

Fig. 20. Rotor position estimation curve.

TABLE I. PARAMETERS OF THE PMSM

Symbol	Name	Value and Unit
n_p	Machine pole pairs	5
p	Rated power	400W
n	Rated speed	3000r/min
R_s	Stator resistance	1.55Ω
φ_f	Rotor flux linkage	47mWb
L_s	dq-axis inductances	6.71mH
J	Inertia	27.7 kg m^2
J/B	Mechanical constant	0.53

TABLE II. PARAMETERS OF THE CONTROL METHODS

Name	Value
The gains of SMC	$c=100$, $q=300$ $\varepsilon=200$
The gains of improved SMC	$c=200$, $\alpha=2$ $q=300$, $\varepsilon=200$
The gains of traditional NTSMC + traditional attractor	$p=9$, $q=7$, $\beta=100$, $\phi=50$, $\gamma=30$, $m=3$, $n=5$
The gains of NFTSMC+ improved attractor	$p=9$, $q=7$ $g=7$, $h=5$, $c=1000$ $\beta=1$, $\alpha=100$ $\phi=50$, $\gamma=30$ $m=3$, $n=5$

shortcomings of large jitters in the commonly used symbol-switching functions in variable structures, a variable-structure MRAS observer with continuous hyperbolic tangent function sigmoid as the switching function is designed. It is applied to the PMSM vector control system without a speed sensor. Both the simulation and experimental results verify that the SM-MRAS system has good tracking performance under conditions such as sudden load changes and changes in internal parameters of the motor. In order to comprehensively solve the singularity and chattering problems of SMC and improve its convergence speed, a nonsingular fast terminal sliding mode speed-control scheme with exponential terminal attractors is proposed. Compared with the traditional sliding mode control, the motor speed error can converge to the equilibrium point faster, the control variable chattering is small, the speed steady-state accuracy is high, and it has strong robustness to load disturbances and parameter disturbances. Simulation analysis and experimental research results show the feasibility and effectiveness of the control scheme.

The main idea of MRAS is to select the equation with parameters to be estimated as the adjustable model and the equation without unknown parameters as the reference model, and the two models have the same physical meaning of the output. The output value of the reference model is taken as the ideal response, and then the parameters of the adjustable model are adjusted in real time by the

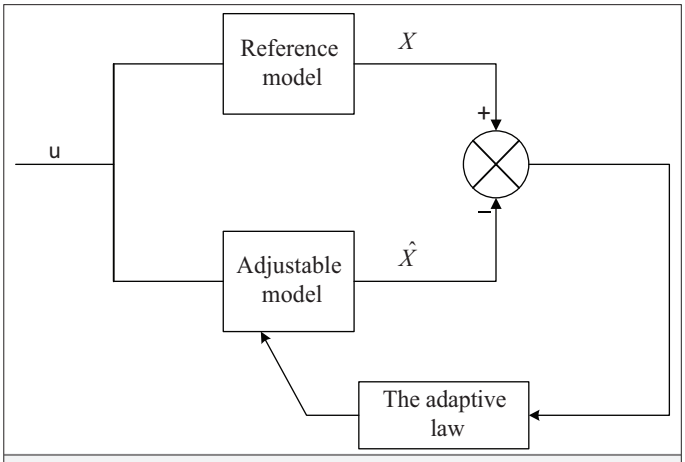

Figure 21. Schematic diagram of MRAS

appropriate adaptive law, so that the output difference between the two models approaches zero, so that the output of the control object can track the output of the reference model. Schematic diagram of MRAS is shown in Fig. 21.

The selection of reference model and adjustable model should meet the following requirements: the equation of reference model does not contain parameters to be estimated, while the adjustable model contains parameters to be estimated. The matrix equation of the reference model is as follows:

$$\begin{cases} X_m = A_m X_m + B_m u \\ X_m(0) = X_{m0} \end{cases} \tag{41}$$

In Equation (41), X_m is the n-dimensional state vector, u is the m-dimensional input vector, A_m and B_m are the m-dimensional constant matrix. The matrix equation of the adjustable model can be expressed as:

$$\begin{cases} X_s = A_s(t) X_s + B_s(t) u \\ X_s(0) = X_{s0}, A_s(0) = A_{s0}, B_s(0) = B_{s0} \end{cases} \tag{42}$$

In Equation (42), X_s is the n-dimensional state vector, $A_s(t)$ and $B_s(t)$ are constant matrices that change with time. The mathematical expression of generalized error can be obtained from Equation (41) and Equation (42) :

$$e = X_m - X_s \tag{43}$$

For the design of adaptive law of model reference adaptive, it is necessary to make the generalized error E adjust parameter matrix $A_s(t)$ and $B_s(t)$ according to certain law. Finally, let the generalized error e approach zero. Considering the stability of the identification system to ensure state convergence, the integration function of memory function should be included, and the adjustable parameter is not only dependent on the current generalized error value, but also related to its past value. So, the adaptive equation is as follows.

$$\begin{cases} A_s(t) = \int_0^t F_1[v, \tau, t] d\tau + F_2[v, t] \\ B_s(t) = \int_0^t G_1[v, \tau, t] d\tau + G_2[v, t] \end{cases} \tag{44}$$

In the formula, $v \neq De$, D is a linear compensator, and the adaptive rate of the system is determined by generalized error. In order to achieve a completely progressive adaptation, any initial conditions need to be satisfied. The equation of generalized error e can be obtained from Equation (44) as follows,

$$\begin{aligned} e = A_m e + \left\{ \left[A_m - A_s(0) - \int_0^t F_1(v, \tau, t) d\tau - F_2(v, t) \right] X_s \right. \\ \left. + \left[B_m - B_s(0) - \int_0^t G_1(v, \tau, t) d\tau - G_2(v, t) \right] u \right\} \end{aligned} \tag{45}$$

Let the right side of Equation (45) be equal to W_1, and the adaptive equation can be obtained as shown in Equation (46)

$$\begin{cases} e = A_m e + W_1 \\ v = De \\ W = -W_1 \end{cases} \tag{46}$$

According to Equation (46), it can be concluded that the equivalent system consists of two parts, the linear part and the nonlinear feedback part.

According to the mathematical model of permanent magnet synchronous motor, the formula (5) is selected as the reference equation of MRAS, and the formula (7) is selected as the adjustable equation of MRAS. The adaptive rate of rotational speed is deduced through Popov super-stability theory, so as to obtain the position and speed information of the rotor of the motor.

The extended state observer (ESO) can estimate unknown disturbances in real time with high accuracy. ESO borrows the idea of state observer, expands unknown disturbance variable into new state variable, and uses special feedback mechanism to establish a new observer that can observe the expanded state. The implementation of ESO is as follows.

For the following first order system,

$$\begin{cases} \dot{x} = f_0 + f_1 + b_0 u \\ y = x_1 \end{cases} \tag{47}$$

In the formula, x is the state variable, f_0 is the known mode of the system, f_1 is the unknown mode of the system, b_0 is the input amplification coefficient, u is the control input, and the expression quantity of the unknown mode f_1,

$$a(t) = f_1 \tag{48}$$

When a new unknown state variable is added to the original system, the original system can become,

$$\begin{cases} \dot{x}_1 = f_0 + x_2 + b_0 u \\ \dot{x}_2 = f_1 = a(t) \\ y = x_1 \end{cases} \tag{49}$$

For this system, we can design a linear ESO of the following form,

$$\begin{cases} e = z_1 - y \\ \dot{z}_1 = z_2 + f_0 + b_0 u - \beta_1 e \\ \dot{z}_2 = -\beta_2 e \end{cases} \tag{50}$$

Where, z_1 is used to observe the output y, while z_2 is used to observe the unknown mode f_1 of the system.

Peer-review: Externally peer-reviewed.

Author Contributions: Concept – Q.A., Y.C.; Design – Q.A., Y.C.; Supervision – Q.A., Y.C.; Resources – Q.A., Y.C.; Materials – Q.A., Y.C.; Data Collection and/or Processing – Q.A., Y.C.; Analysis and/or Interpretation – Q.A., Y.C.; Literature Search – Q.A., Y.C.; Writing Manuscript – Q.A., Y.C.; Critical Review – Q.A., Y.C.

Declaration of Interests: The authors declared that they have no conflict of interest.

Funding: The authors declared that the study has received no financial support.

REFERENCES

1. X. G. Zhang, K. Zhao, L. Sun, and Q. T. An, "A new approach rate control for permanent magnet synchronous motor sliding mode variable structure speed regulation system," *Proc. Chin. Soc. Electr. Eng.*, vol. 31, no. 24, pp. 77–82, 2011. [CrossRef]
2. Y. Lei, B. X. Hu, K. Y. Wei, and S. Chen, *Modern Permanent Magnet Synchronous Motor Control Principles and MATLAB Simulation*. Beijing, China: Beijing University of Aeronautics and Astronautics Press, 2016, p. 3.
3. Y. Liu, J. Zhao, M. Xia, et al., "Model reference adaptive control-based speed control of brushless DC motors with low-resolution hall-effect sensors," *IEEE Trans. Power Electron.*, vol. 29, no. 3, pp. 1514–1522, 2016. [CrossRef]
4. V. Ruuskanen, J. Nerg, M. Rilla, and J. Pyrhonen, "Iron loss analysis of the permanent-magnet synchronous machine based on finite-element analysis over the electrical vehicle drive cycle," *IEEE Trans. Ind. Electron.*, vol. 63, no. 7, pp. 4129–4136, 2016. [CrossRef]
5. Z. H. Deng and X. H. Nian, "Robust control of permanent magnet synchronous motors," *IEEE CAA J. Autom. Sin.*, vol. 2, no. 2, pp. 143–150, 2015.
6. H. Wang, S. Li, Q. Lan, Z. Zhao, and X. Zhou, "Continuous terminal sliding mode control with extended state observer for PMSM speed regulation system," *Trans. Inst. Meas. Control*, vol. 39, no. 8, pp. 1195–1204, 2017. [CrossRef]
7. Y. Yi, D. Vilathgamuwa, and M. Rahman, "Implementation an artificial-neural-network-based real-time adaptive controller for an interior permanent-magnet motor drive," *IEEE Trans. Ind. Appl.*, vol. 1, no. 39, pp. 96–104, 2003. [CrossRef]
8. Y. Li and Y. Chen, "The Research of Gain Adaptive Linear Extended State Observer (ALESO) based active disturbance rejection speed control for permanent magnet synchronous motor," *Electrica*, vol. 21, no. 1, pp. 20–31, 2021. [CrossRef]
9. V. Utkin, "Variable structure systems with sliding modes," *IEEE Trans. Autom. Control*, vol. 22, no. 2, pp. 212–222, 1977. [CrossRef]
10. J. Y. Hung, W. Gao, and J. C. Hung, "Variable structure control: a survey," *IEEE Trans. Ind. Electron.*, vol. 40, no. 1, pp. 2–22, 1993. [CrossRef]
11. Y. Feng, X. H. Yu, and Z. H. Man, "Non-singular terminal sliding mode control and its application for robot manipulators," in *Proceedings of the IEEE International Symposium on Circuits and Systems*. Piscataway, NJ, USA: IEEE Publications, 2001, pp. 545–548. [CrossRef]
12. W. Xu, Y. Jiang, C. Mu, and H. Yue, "Nonsingular terminal sliding mode control for the speed regulation of permanent magnet synchronous motor with parameter uncertainties," in *IECON 2015 – 41st Annual Conference of the IEEE Industrial Electronics Society*, 2015, pp. 1994–1999.
13. S. S. Xu, C. Chen, and Z. Wu, "Study of nonsingular fast terminal sliding mode fault-tolerant control," *IEEE Trans. Ind. Electron.*, vol. 62, no. 6, pp. 3906–3913, 2015. [CrossRef]
14. B. Xu, X. Shen, W. Ji, G. Shi, J. Xu, and S. Ding, "Adaptive nonsingular terminal sliding model control for permanent magnet synchronous motor based on disturbance observer," *IEEE Access*, vol. 6, pp. 48913–48920, 2018. [CrossRef]
15. S. Cao, J. Liu, and Y. Yi, "Non-singular terminal sliding mode adaptive control of permanent magnet synchronous motor based on a disturbance observer," *J. Eng.*, vol. 2019, no. 15, pp. 629–634, 2019. [CrossRef]
16. X. Yu and M. Zhihong, "Fast terminal sliding-mode control design for nonlinear dynamical systems," *IEEE Trans. Circ. Syst. I Fund. Theory Appl.*, vol. 49, no. 2, 2002, pp. 261–264. [CrossRef]
17. W. Xu, A. K. Junejo, Y. Liu, and M. R. Islam, "Improved continuous fast terminal sliding mode control with extended state observer for speed regulation of PMSM drive system," *IEEE Trans. Veh. Technol.*, vol. 68, no. 11, pp. 10465–10476, 2019. [CrossRef]
18. K. Junejo, W. Xu, C. Mu, and Y. Liu, "Improved fast terminal sliding mode control for speed regulation of surface-mounted permanent magnet synchronous motor," in *21st International Conference on Electrical Machines and Systems (ICEMS)*, Vol. 2018, 2018, pp. 93–98.

Qiao Ai received her bachelor's degree in engineering from Yangtze University, Hubei province, China, in 2020. She is currently studying for her Master's degree at Yangtze University, Hubei Province, China. Her main research interests include electronics and electrical transmission, and sliding mode control.

Yongjun Chen is associate dean, professor, PhD, and master tutor of the School of Electronic Information, Yangtze University. He is a senior visiting scholar at Aalborg University in Denmark, where his research interests include power electronics, electrical drives, and the control of special motors.